Enabling Emerging Applications in 5G Through UE-Assisted Proactive PHY Frame Configuration

Moinak Ghoshal*, Subhramoy Mohanti†, Dimitrios Koutsonikolas*
*Northeastern University, USA
†InterDigital Communications, Inc., USA
Email: ghoshal.m@northeastern.edu, subhramoy.mohanti@interdigital.com, d.koutsonikolas@northeastern.edu

***Abstract*—Ubiquitous connectivity is vital for emerging applications like extended reality, factory automation, and robotics, necessitating low latency, high data rates, and reliability in both downlink and uplink. From the network protocol perspective, successfully supporting these new use cases hinges on the network being resilient enough to address the heterogeneous demand in dynamic channel conditions. To assess the performance of legacy 5G networks for these applications, we focus on the physical (PHY) layer and analyze the existing 5G time division duplexing (TDD) method in terms of throughput. Our preliminary experiments with 3rd Generation Partnership Protocol (3GPP) compliant Matlab 5G toolbox reveal limitations of the *fixed* configuration of the PHY frames, that are typically used by commercial 5G networks, hindering adaptability to heterogeneous demands and compromising quality of service (QoS). To overcome this, we propose a machine learning-enabled optimization framework facilitating proactive PHY frame reconfiguration based on real-time *prediction* of wireless channel metrics computed at User Equipment (UE). Implementation and validation of our approach on the 3GPP-compliant Open Air Interface (OAI) 5G testbed demonstrate the practicality of our solution and its adherence to 3GPP standards. Overall, our dynamic PHY frame configuration approach consistently meets overall traffic demands better than any fixed configuration across various scenarios, while also having the lowest percentage of un-transmitted bytes in each scenario.**

I. Introduction

5G technology promises to support a wide range of emerging applications in the near future, from immersive extended reality experiences to machine-type applications like networked robotics [1], [2]. These applications can offload tasks such as object detection/recognition/tracking to edge servers [3], thereby presenting a distinctive array of challenges. This methodology demands high uplink throughput and imposes stringent requirements in terms of latency and reliability [4], [5] which are pivotal for ensuring seamless communication over wireless links, particularly in scenarios characterized by mobility and high user density [6]. To ensure adherence to application QoS thresholds, 3GPP provides the flexibility of selecting a PHY frame configuration, comprising of a specific number of downlink (DL) and uplink (UL) slots in the time domain, from a range of available options [7], [8], to aid time-domain resource allocation. This process is managed by the Network (NW), encompassing both the base station (gNB) and the core network (CN).

• **Bridging the gap in 5G:** Allocation of the DL/UL slots in a PHY frame among available UEs is achieved through time division duplexing (TDD). Here, the NW relies on UE reports of estimated wireless channel conditions, pending application traffic for the UEs, and their QoS requirements to determine the allocation of UEs to specific DL or UL slots in a PHY frame, along with UE transmission configurations like MCS [9]. This *reactive* approach may exhibit sluggish convergence to an optimal PHY frame configuration, along with optimal UE allocation to DL/UL slots, and MCS selection in dynamic environments characterized by high variance in channel metrics such as SINR, RSRP, RSSI. This potentially increases the likelihood of failing to meet the QoS thresholds for emerging applications. Commercial 5G networks get around this problem by having a *fixed* PHY frame configuration with more DL slots than UL [10], giving more priority to existing DL-heavy applications like video streaming, and resulting in a noticeable performance gap between the DL and UL in terms of throughput [6]. While various factors contribute to this asymmetry, the reactive scheduling by the NW, particularly the lack of updates to DL and UL slot configurations in the PHY frame based on user demands and channel conditions, plays a significant role.

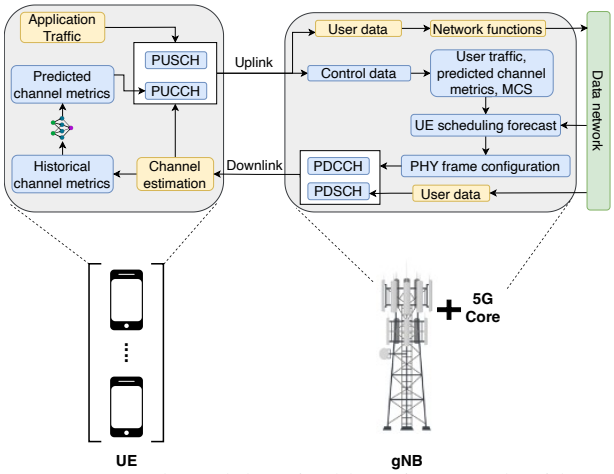

Fig. 1: Proposed modules (in blue) integrated with 3GPP compliant 5G network modules (in yellow) for proactive UE time domain resource allocation.

• **Proposed framework description:** We explore the possibility of addressing the aforementioned gaps in 5G by investigating *proactive* PHY frame reconfiguration. Here, the number of DL and UL slots in a PHY frame is decided based on the real-time application traffic demand and *predictions* of the UE channel metrics. We propose an adaptive and autonomous UE-based machine learning (ML)-enabled solution, that allows

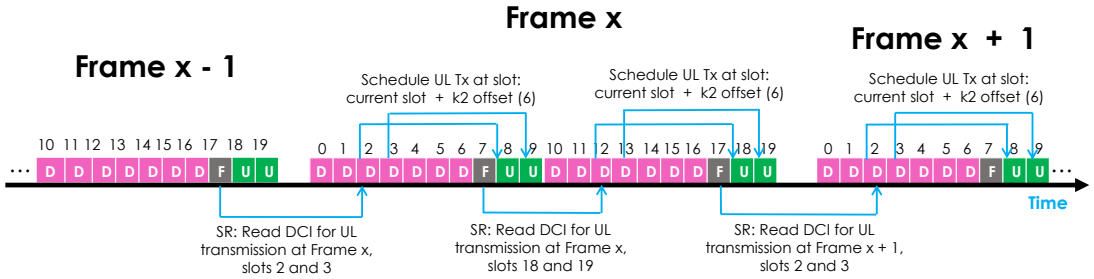

Fig. 2: Uplink transmission process in legacy 5G PHY TDD frame configuration with 30 KHz sub-carrier spacing

the UEs to predict their local channel metrics for future time instances, and report them to the NW. This *lookahead* from all the available UEs can enable the NW to proactively configure the DL and UL slots for future PHY frames and pre-allocate UEs to these slots to meet the diverse application requirements in dynamic channel conditions. While the NW can store channel metric data from all served UEs, executing ML algorithms on each UE's reported channel data for real-time forecasting is not scalable from the NW side. A more practical approach is for individual UEs to forecast their channel metrics and transmit them to the NW, facilitating proactive resource optimization.

Our solution is designed to operate with the existing 3GPP standard with added enhancements shown in Fig. 1: (i) Deployed UEs with trained machine learning (ML) modules for local channel metric prediction, that are reported to the NW along with the application traffic demand, and (ii) the optimization suite in the NW, which receives this forwarded information from the UEs and proactively reconfigures the PHY frame with an optimal number of DL and UL slots. This helps to allocate UEs to the best possible slots in the PHY frame and maintain the QoS requirement.

The main contributions of the paper are as follows:

- We leverage 3GPP-compliant Matlab 5G toolbox [11], to characterize how legacy 5G allocates UEs in the PHY frame in the time domain based on UE reported channel metrics, and motivate how this approach can be a bottleneck for emerging UL-heavy applications.
- We introduce a proactive PHY frame configuration framework enabling dynamic allotment of DL and UL slots in a PHY frame through *look-ahead forecasts* of UE channel metrics and application demand, enhancing network QoS compared to reactive resource allocation. Crucially, our framework is straightforward and aligns with the 3GPP standard.
- We deploy our proposed method on the 3GPP-compliant OAI 5G testbed [12] to showcase its practicality and adherence to 3GPP standards. By comparing our solution with the baseline reactive legacy 5G TDD, through both testbed experiments and simulations, we demonstrate an enhanced equilibrium between DL and UL performance. These findings underscore the critical role of proactive PHY frame reconfiguration in accommodating the diverse demands of emerging applications within dynamic channel environments.

II. Background and Motivation

3GPP employs dynamic scheduling to allocate resources to UEs in the time domain, representing the prevalent method in commercial cellular networks [10]. Our proposed solution builds upon this approach, aiming to enhance its efficacy.

A. Legacy 5G dynamic scheduling

Commercial 5G networks such as AT&T, T-Mobile, and Verizon all configure the 5G PHY frame of 10 ms duration, with the same *fixed* configuration that has more DL than UL slots – 7 DL-2 UL-1 F (7 DL 3 UL) [13], with a periodicity of 5 ms, as shown in Fig. 2, leading to imbalanced traffic distribution. With this frame configuration, the UE triggers the dynamic scheduling process by transmitting a Scheduling Request (SR) to the NW in a UL or F slot, indicating pending UL data, and providing channel estimates via the physical uplink control channel (PUCCH) [14]. Subsequently, the NW informs the UEs of resource allocation using downlink control information (DCI) in the downlink control channel (PDCCH). Here, among other things, the NW specifies slot assignments for UEs in the uplink service channel (PUSCH) and downlink service channel (PDSCH) for UL transmission and DL reception, respectively.

Existing drive-test studies on these commercial networks using 5G smartphones reveal impressive DL speeds, surpassing 3.5 Gbps, while UL throughput remains consistently lower [6]. The fixed DL-heavy PHY frame configuration may strain 5G networks, particularly with the rise of uplink-heavy applications. The use of this fixed PHY frame configuration persists due to the prevalence of existing DL-heavy applications and the 3GPP-supported *reactive* scheduling method based on UE-reported channel metrics. The lack of channel forecast knowledge provides little incentive for the NW to modify PHY frame configuration relying solely on UE-reported channel metrics as this process may take time to converge and can result in sub-optimal NW performance.

B. Preliminary Experiment and Observation

To further quantify the limitations of different fixed PHY frame configurations on UL-heavy applications, we conducted controlled experiments with the 3GPP-compliant Matlab 5G toolbox. The experiment featured a gNB and a UE connected via the 900 MHz frequency in SISO configuration, with 40 MHz BW and 30 KHz subcarrier spacing (SCS). We simulated typical UL and DL communication using on-off application traffic with no mobility, thereby ensuring stable channel conditions to specifically assess the impact of PHY

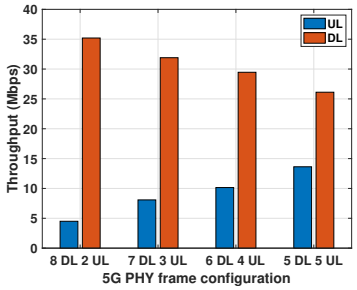

Fig. 3: Imbalanced throughput distribution between UL and DL with different 5G PHY frame configurations

frame configurations on UE throughput. Utilizing flexible (F) slots as UL slots, as per 3GPP standard, we measured throughput in UL and DL with various PHY frame configurations: 8 DL 2 UL, 7 DL 3 UL, 6 DL 4 UL, and 5 DL 5 UL.

The results from the experiments are shown in Fig. 3. Here, we observe UL throughput of ∼8 Mbps for the 7 DL 3 UL configuration, ∼10 Mbps for the 6 DL 4 UL configuration, ∼4.5 Mbps for the 8 DL 2 UL configuration and ∼14 Mbps for 5 DL 5 UL configuration. DL throughput ranged between 25 - 35 Mbps in these frame configurations. These results underscore a clear inverse relationship between DL-heavy PHY frame configurations and UL throughput. Note that the UL to DL throughput ratio does not exactly follow the slot allocation ratio for two reasons: First, for UL transmissions, the UE utilizes one whole F/mixed slot to send a scheduling request to notify the NW regarding incoming UL data transmission in the upcoming frame cycle. Second, in 3GPP for a given MCS, the maximum data transport block size for DL is higher compared to UL [9], leading to such asymmetry in throughput.

III. Proactive PHY frame configuration

We now elaborate on how our proposed solution facilitates the proactive selection of PHY frame configuration with active UE assistance. The overall system diagram for this process is depicted in Fig. 4. Here, the UE reports the most recent channel estimates to the NW (legacy method) and also predicts/forecasts the channel related metrics such as SINR, RSRP, RSSI, etc., through local AI/ML models, by using historical channel metric data as input and transmits it along with the application traffic status to the NW in the UL. The NW on receiving this information from multiple UEs, computes the preferred resource allocation metrics (e.g., slot/symbol, MCS, etc.), and proactively configures future frames with slots that cater to the needs of all the UEs, while minimizing interference to neighbor cells, thus optimizing the overall performance of the network. This information is communicated to the UE via legacy time domain resource allocation. We next describe how UE channel metric prediction helps in time domain resource allocation, through proactive PHY frame configuration.

A. UE Channel Metric Prediction

In UEs that support channel metric prediction, the process is as depicted in Fig. 5. Here, each UE keeps a record of the historical channel metric data in a local buffer. At the

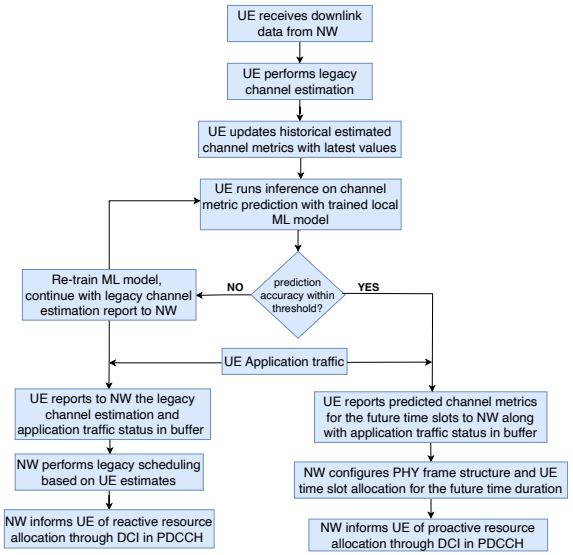

Fig. 4: Dynamic PHY frame reconfiguration at NW aided by UE forecast of local channel metrics.

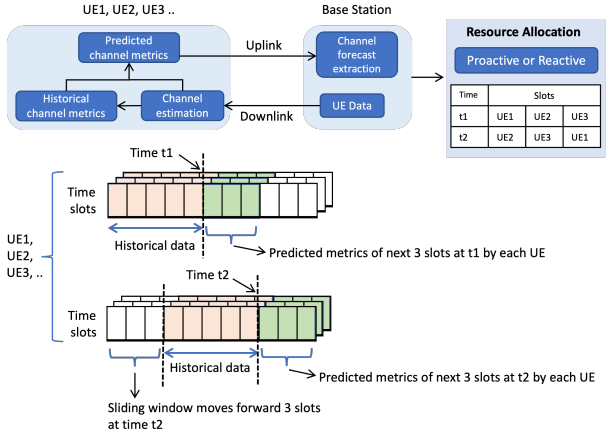

Fig. 5: Sliding window mechanism at UE in using historical channel metrics (in orange) to predict the channel metrics of future time slots (in green).

beginning of time $t1$, the UE uses this historical channel metric data as input for the channel metric prediction module, which forecasts channel metrics for a desired number of time slots in the future by leveraging Long Short Term Memory (LSTM) neural networks, a type of recurrent neural network (RNN) specifically designed to capture and analyze sequential data. This forecast data is then shared with the NW by each UE through the UL. The NW can use this forecast knowledge to proactively allocate network resources in the time and frequency domains to the UEs. This resource allocation information is then communicated back to the UEs through the DL channel. At time instant $t2$, to predict the next batch of channel metrics, the UEs follow a sliding window mechanism, as shown in Fig. 5. This allows the UEs to use the most recent historical data, for the prediction module. At the next cycle of channel metric prediction (time $t2$), this window moves forward by the number of time slots for which the channel metrics are predicted (e.g., 3 slots in Fig. 5). At every time slot,

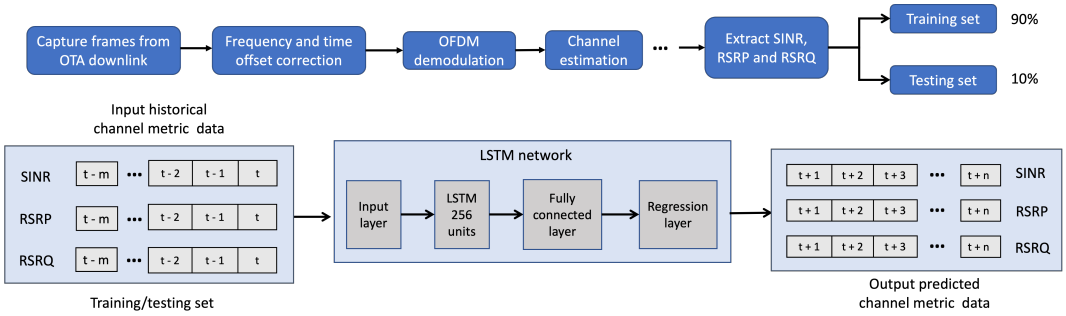

Fig. 6: Tensor forming, training and testing processes in the proposed LSTM network for UE channel metric prediction. The SINR, RSRP and RSRQ sequences are divided into training, and testing sets, which are used for channel metric prediction.

the UEs verify how far the predicted channel metric values fall from the actual estimated value for that time slot. This prediction accuracy is important since lower accuracy means false channel metric prediction, which can affect the UE QoS. For this reason, the UEs can revert to legacy reactive resource allocation and re-trains the ML model, if the predicted value crosses a predefined accuracy threshold metric (Fig. 4).

• **LSTM based prediction:** The capability of deep learning methods to identify complex, non-linear patterns in data makes them ideal for time series forecasting [15], [16]. Among the available methods, Long Short-Term Memory (LSTM) has been successfully applied in a range of different domains, including aspects of wireless network infrastructure management [17]. Despite the widespread adoption of machine learning architectures like Transformers for time series prediction tasks, their extensive parameterization, substantial memory footprint, and computational demands render them unsuitable for deployment on resource-constrained low-power devices such as UEs [18]. Given our study's focus on leveraging accurate time series predictions to guide proactive design strategies for 5G PHY frame configurations and support emerging UL-intensive applications, we select LSTM networks as an exemplary, demonstrative, and cost-effective approach.

The LSTM architecture that we use for UE channel metric prediction is depicted in Fig. 6. Given an input of historical time series or sequence ($t-m$ to t) of channel metric data, the LSTM network forecasts the channel metric values of future time steps $t+1$ to $t+n$, with $t+n$ being the forecast time horizon. We measure the accuracy of the predictions through Root Mean Square Error (RMSE) $\mathcal{E}$, which shows how far the predictions fall from measured true values using Euclidean distance, and it is expressed as $\mathcal{E} = \sqrt{\frac{\sum_{t=1}^{\mathcal{N}} \|x_t - \hat{x}_t\|^2}{\mathcal{N}}}$ where, $\mathcal{N}$ is the number of data points, x_t is the measurement at time t, and $\hat{x}_t$ is its corresponding prediction. For accurate prediction, we set the RMSE threshold to 1. Fig. 7 shows the performance of the LSTM network in predicting the channel metrics for 1 future frame and 10 future frames with input channel metric data of 400 previous frames collected from over-the-air drive test experiments, with the channel metrics having a granularity of 10 ms.

B. Proactive Time Domain Resource Allocation

We next describe the algorithm designed to address the proactive time domain resource allocation between two UEs,

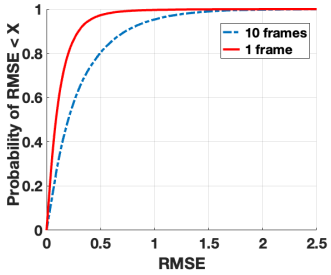

Fig. 7: RMSE of LSTM for predicting channel metrics for duration of 1 and 10 frames with input historical channel metric data of 400 previous frames.

aided by the UE channel metric prediction in a 5G network with stringent latency requirements. The resource allocation algorithm tries to choose a frame configuration per TDD PHY frame which maximizes the total throughput of a network. On the UE side, once the channel metric prediction module provides a series of SINR values for the next prediction window, the UE maps it to an MCS from the channel quality indicator (CQI) table and fetches the corresponding maximum achievable Transport Block Size (TBS), per slot in each frame, for the duration of the forecast time. The forecast time corresponds with the considered latency deadline (e.g., 20 ms, 100 ms). These predicted channel metrics, application buffer status, and the TBS values are then sent to the NW via the PUCCH at the beginning of every resource allocation period. The resource allocation is triggered by the arrival of application traffic at the UE buffer. The NW, upon receiving the list of TBS from the two UEs, runs the PHY frame configuration algorithm to perform the proactive UE resource allocation. Since our goal in this work is to demonstrate the benefits of proactive PHY frame configuration and not to propose an optimal scheduling algorithm, we describe a simple algorithm assuming that there are two UEs in the network (UE1 and UE2), and they are using UL-centric and DL-centric applications respectively.

We initialize each UE's traffic demands in the current prediction window and assign the frame configurations for the number of frames that cover the prediction window, with each frame having 10 ms duration. For each frame, our algorithm calculates the sum of DL (UE2) and UL (UE1) TBS, for all possible allowed PHY frame configurations ranging from (1 DL 9 UL), (2 DL 8 UL), to (9 DL 1 UL). Note, when both

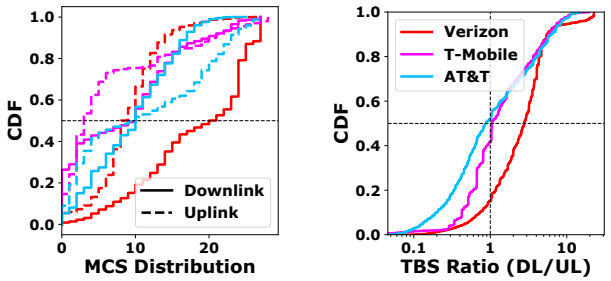

(a) 5G MCS distribution (b) Ratio of DL to UL TBS per slot

Fig. 8: MCS and DL to UL TBS ratio distribution in mobility scenarios for all 3 operators.

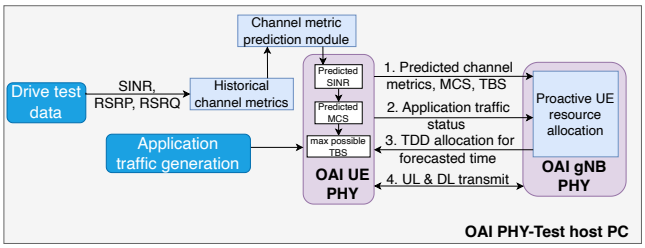

Fig. 9: Schematic diagram of proactive PHY frame configuration in OAI by leveraging drive test data

the UE's traffic demands cannot be satisfied within the latency deadline due to poor channel conditions, the algorithm never chooses an extreme frame configuration like (10 DL 0 UL) or (0 DL 10 UL), even if that frame configuration maximizes the network throughput. This ensures none of the UEs get starved until their traffic demands are satisfied. The sum TBS of the two UEs acts as a proxy to the total network throughput. The algorithm then chooses the frame configuration with the maximum sum TBS value and assigns that configuration to the current frame. The allocated TBS per UE is then deducted from the traffic demands of both the UEs respectively. The algorithm then checks if the UEs' traffic demands are satisfied in the current frame configuration cycle. If both the UE's traffic demands are satisfied, then the remaining frames are assigned an equal distribution of DL and UL slots (5 DL 5 UL). If either of the UE's requirements gets satisfied first, then for the remainder of the frames within the latency deadline, the other UE is allocated all the slots needed to finish its task; (10 DL 0 UL) for the DL UE or (0 DL 10 UL) for the UL UE. After allocating the slots in each PHY frame for the duration of the prediction window (latency deadline), the NW sends the indication of allocated slots to the UEs via legacy DCI in PDCCH.

IV. Performance Analysis

We explore the performance gain of our proposed solution by leveraging channel metrics collected from outdoor drive tests using 5G-enabled commercial smartphones.

A. Experiments

The outdoor drive test dataset is a collection of cellular channel metrics and packet traces collected from Samsung S21 smartphones (UEs) during different outdoor drive test settings. Each of the UEs run the XCAL Solo tool [19], which provides low-level access to detailed cellular signal metrics and protocol information. Each of the UEs was equipped with SIM cards of one of the major US network operators (Verizon, T-Mobile, AT&T) and we conducted extensive drive test campaigns in a major city in the US. During each of these tests, the UEs continuously ran backlogged traffic using iperf. The dataset obtained here is a time series of channel metrics (SINR, CQI, RSRP, etc.) having a granularity of 10 ms. The goal of this dataset is to capture *realistic*, *mobile* settings in which a typical UE might operate as seen in Fig. 8a which shows how drastically the 5G MCS can fluctuate under mobility for all three operators. We observe that with the exception of AT&T, where 50% of the time the UL MCS was higher than the DL MCS and vice-versa, the other two operators had higher DL MCS dominating most of the time. We also calculated the ratio between each 10 ms DL and UL max TBS sample extracted at the same time instant and show it in Fig. 8b. Unsurprisingly, for Verizon, due to its extremely DL-heavy MCS distribution (9 vs. 21 median UL and DL MCS respectively), the TBS ratio is more than 1 most of the time. For AT&T and T-Mobile we see a much more balanced distribution of the DL to UL TBS ratio.

We integrate the drive test channel metric data (SINR, MCS) to the OAI testbed, running in PHY-test mode [12], with added customizations as explained in Sec. III.B, to enable the dynamic PHY frame configuration without requiring the assistance of the upper layers of the network stack. The schematics for this experiment are shown in Fig. 9, where the forecasted channel metrics are transmitted to the NW via the UE for proactive PHY frame configuration. Following the gNB indication of UE resource allocation in the DL, the UE starts the UL and DL transmission. The PHY layer logs capturing the UE and gNB interaction are used for performance evaluation.

We ran the OAI-PHY test mode using each of the traffic traces collected from the drive tests for 2 different PHY frame configurations: (a) Previously explained static configurations, which remained constant from start to end of a run: (5 DL 5 UL), (6 DL 4 UL), (7 DL 3 UL), and (8 DL 2 UL), and (b) Dynamic configuration, which lets the NW choose different frame configurations for each frame depending on the traffic requirements and predicted channel quality. For the latency thresholds, we choose the emerging applications of intelligent transportation (100 ms) and machine-type communication (20 ms) [5], with traffic arrival rate at 100 ms and 20 ms respectively. In this scenario, even though our system can dynamically configure each frame with different DL and UL slots, due to OAI constraints we are only allowed to choose among the 4 configurations mentioned in the static scenario. To fully realize the potential of dynamic PHY frame configuration with DL and UL slots, we also run offline simulations where the OAI constraints do not restrict the frame configuration algorithm and it selects the per-frame configuration (among all possible configurations) that maximizes the throughput. We define this as the *dynamic-nonOAI* scenario and the previous dynamic scenario bounded by OAI constraints as *dynamic-OAI*.

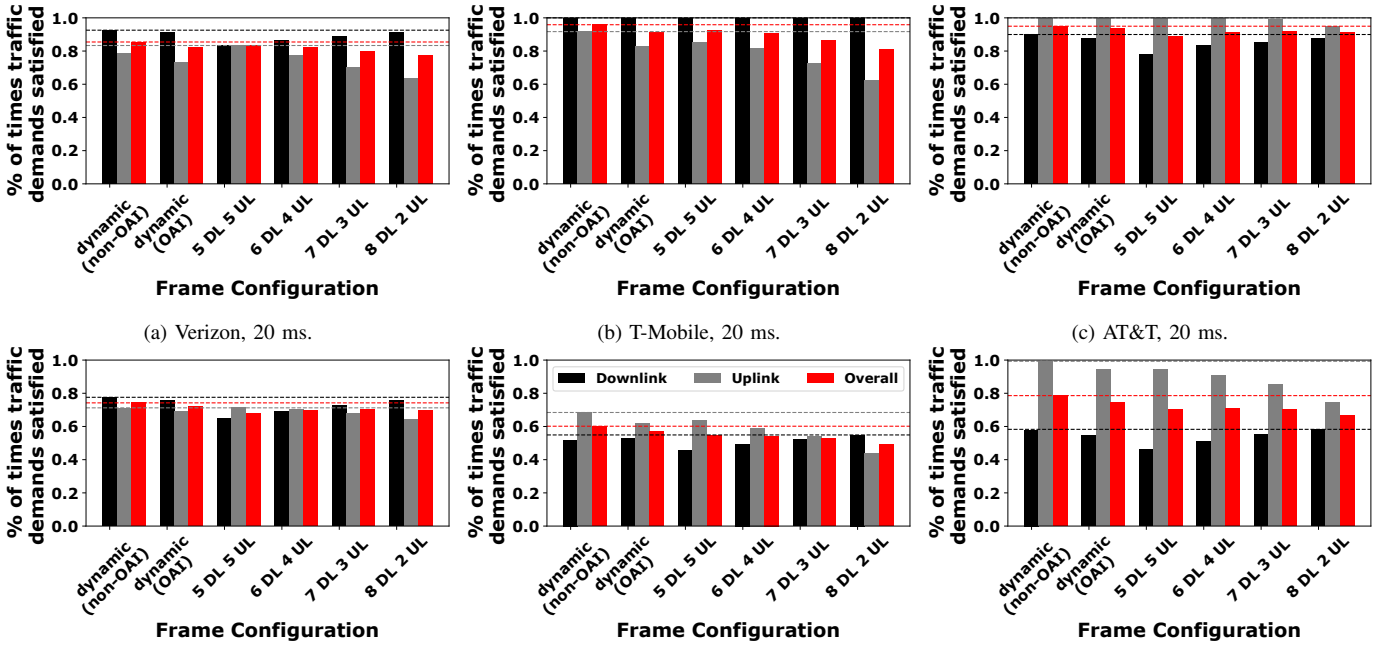

(a) Verizon, 20 ms. (b) T-Mobile, 20 ms. (c) AT&T, 20 ms.

(d) Verizon, 100 ms. (e) T-Mobile, 100 ms. (f) AT&T, 100 ms.

Fig. 10: % times the DL and UL traffic demands were satisfied with different PHY frame configurations for 20 ms and 100 ms latency deadlines.

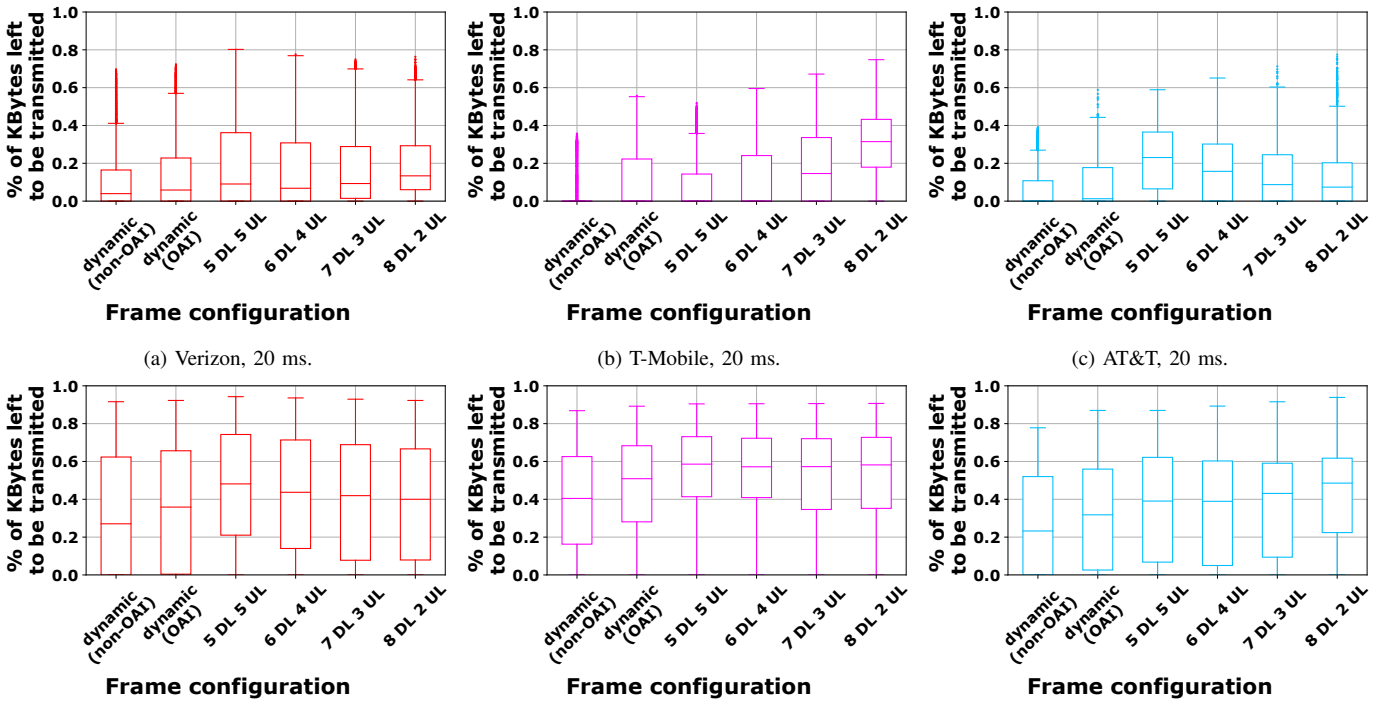

(a) Verizon, 20 ms. (b) T-Mobile, 20 ms. (c) AT&T, 20 ms.

(d) Verizon, 100 ms. (e) T-Mobile, 100 ms. (f) AT&T, 100 ms.

Fig. 11: % of total DL + UL untransmitted traffic with respect to the traffic demand in a 20 ms and 100 ms interval for the cases where the traffic demand was not satisfied within its deadline in at least one direction.

In the experiments, we perform channel metric prediction and dynamic PHY frame configuration for a window of 100 ms (10 frames) and 20 ms (2 frames) emulating the behavior of emerging applications. Accordingly, based on the application type and the maximum capacity of our network, we choose the maximum traffic for each of the cases. For the application with 100 ms latency, we set the maximum traffic generated per 100 ms cycle as 62.5 KB, and for the application with 20 ms

latency, we set the maximum traffic to be 9.5 KB for 20 ms.

B. Results

For each of the frame configuration types: *static*, *dynamic-OAI*, and *dynamic-nonOAI*, we evaluate the efficacy of each type using two metrics: a) % of times the traffic demand in a 20 ms or 100 ms latency deadline cycle was satisfied using a specific frame configuration type (the higher the better), and b) % of remaining bytes that could not be transmitted within the latency deadline for the cases where the traffic demand was not satisfied within its deadline in at least one direction (the lower, the better).

Fig. 10 shows the % of times the traffic demand was satisfied within a 20 ms and 100 ms latency deadline in each direction separately and in total for all three network operators. In general, we observe the dynamic-nonOAI system overall outperforms all other PHY frame configurations. Unlike static configurations, which tend to satisfy the traffic demand requirements in only one direction depending on whether the configuration is DL-heavy or UL-heavy, the dynamic-nonOAI system strikes a balance between both traffic directions by dynamically selecting the best configuration based on predicted traffic demands and channel conditions. As a result, its performance is (i) always better overall than the best static configuration and (ii) either better than or as good as the best static configuration in each direction separately most of the times. Even in the rare cases where a static configuration outperforms the dynamic-nonOAI system in one direction (5DL 5 UL in the UL direction for Verizon with 20 ms latency deadline in Fig. 10a and 8 DL 2 UL in the DL direction for T-Mobile with 100 ms deadline in Fig. 10e), the dynamic nonOAI system offers better overall performance without starving either direction.

We find that these rare cases stem from the channel condition being sometimes substantially poor in a particular traffic direction forcing the resource allocation algorithm to allocate more slots to the other UE with better channel condition. Recall that the resource allocation algorithm tries to maximize the network throughput, thus an asymmetric channel condition will favor the UE with better MCS and finish the task for that UE faster. However, once it notices that a particular UE's task is finished within the expected latency deadline, our algorithm allocates all the remaining resources to the other UE with poor channel condition to complete its task within the latency deadline. This is evident in Fig. 11, which shows that the dynamic-nonOAI is always left with the lowest % of un-transmitted bytes, both in the median and the worst case, in comparison to other frame configurations. In fact, the most symmetric static configuration, 5DL 5 UL, which often achieves comparable performance with dynamic-nonOAI in terms of meeting the latency deadline (Fig. 10), is left with the maximum number of untransmitted bytes in most of the cases (Fig. 11).

In summary, *our dynamic PHY frame configuration satisfies the overall traffic demands more times than any static configuration in every scenario (combination of operator and latency deadline) and, at the same time, it is left with the lowest percentage of un-transmitted bytes in all scenarios.*

V. Conclusion

In our analysis of 5G networks, we uncover limitations in the existing time domain resource allocation approach, which relies on fixed PHY frame configurations derived from UE channel estimates. While effective for prevalent DL-heavy applications, this method struggles with the dynamic and diverse traffic demands of emerging applications spanning both DL and UL. Through extensive experimentation, we demonstrate the superiority of employing proactive PHY frame configurations based on look-ahead forecasting of UE channel metrics to meet application QoS requirements. Our proposed 3GPP-compatible framework maximizes network capacity in both DL and UL, surpassing the performance of legacy DL-heavy PHY frame configurations. This enhancement underscores the importance of precise channel metric prediction in enabling the coexistence of emerging UL-heavy applications with existing DL-heavy applications through efficient time domain resource allocation, leveraging knowledge of current and future channel conditions.

References

[1] I. F. Akyildiz and H. Guo, "Wireless communication research challenges for extended reality (XR)," *ITU Journal on Future and Evolving Technologies*, vol. 3, no. 1, pp. 1–15, 2022.

[2] C. Bai, P. Dallasega, G. Orzes, and J. Sarkis, "Industry 4.0 technologies assessment: A sustainability perspective," *International journal of production economics*, vol. 229, p. 107776, 2020.

[3] L. Liu, H. Li, and M. Gruteser, "Edge assisted real-time object detection for mobile augmented reality," in *ACM MobiCom*, 2019, pp. 1–16.

[4] 3GPP, *Service Requirements for the 5G System, TS 22.261*, 2023.

[5] D. Feng, L. Lai, J. Luo, Y. Zhong, C. Zheng, and K. Ying, "Ultra-reliable and low-latency communications: applications, opportunities and challenges," *Science China Information Sciences*, vol. 64, pp. 1–12, 2021.

[6] M. Ghoshal, I. Khan, Z. J. Kong, P. Dinh, J. Meng, Y. C. Hu, and D. Koutsonikolas, "Performance of cellular networks on the wheels," in *ACM IMC*, 2023, pp. 678–695.

[7] 3gpp, *5G; NR; Physical layer procedures for control, TS 38.213*, 2023.

[8] 3rd generation partnership project (3GPP), *5G NR: Radio Link Control (RLC) protocol specification, TS 38.322*, 2023.

[9] 3GPP, *5G NR Physical layer procedures for data, TS 38.214*, 2023.

[10] R. A. Fezeu *et al.*, "An In-Depth measurement analysis of 5G mmwave PHY latency and its impact on End-to-End delay," in *International Conference on Passive and Active Network Measurement*. Springer, 2023, pp. 284–312.

[11] Mathworks, "5G Toolbox." [Online]. Available: https://www.mathworks.com/help/5g/

[12] OAI, "OAI Run Modem." [Online]. Available: https://gitlab.eurecom.fr/oai/openairinterface5g/-/blob/develop/doc/RUNMODEM.md

[13] R. A. K. Fezeu, J. Carpenter, C. Fiandrino, E. Ramadan, W. Ye, J. Widmer, F. Qian, and Zhi-LiZhang, "Mid-Band 5G: A Measurement Study in Europe and US," Tech. Rep. arXiv:2310.11000v1, 2023.

[14] T. generation partnership project (3GPP), *5G NR: Medium Access Control (MAC) protocol specification, TS 38.321*, 2023.

[15] J. Brownlee, "Time series prediction with LSTm recurrent neural networks in python with keras," *Machine Learning Mastery*, vol. 18, 2016.

[16] F. A. Gers *et al.*, "Learning to forget: Continual prediction with lstm," *Neural computation*, vol. 12, no. 10, pp. 2451–2471, 2000.

[17] M. Chen, U. Challita, W. Saad, C. Yin, and M. Debbah, "Artificial neural networks-based machine learning for wireless networks: A tutorial," *IEEE Communications Surveys & Tutorials*, vol. 21, no. 4, pp. 3039–3071, 2019.

[18] H. Tabani *et al.*, "Improving the efficiency of transformers for resource-constrained devices," in *24th Euromicro Conference on Digital System Design*. IEEE, 2021, pp. 449–456.

[19] Accuver, "XCAL-Solo." [Online]. Available: https://www.accuver.com/sub/products/view.php?idx=48